THE JOURNAL OF BIOLOGICAL CHEMISTRY VOL. 286, NO. 28, pp. 25331–25340, July 15, 2011

Desensitization of α7 Nicotinic Receptor Is Governed by Coupling Strength Relative to Gate Tightness*

Received for publication, January 14, 2011, and in revised form, May 13, 2011 Published, JBC Papers in Press, May 24, 2011, DOI 10.1074/jbc.M111.221754

Jianliang Zhang[‡1], Fenqin Xue[‡1], Paul Whiteaker[‡], Chaokun Li[‡], Wen Wu[§], Benchang Shen[‡¶], Yao Huang[§], Ronald J. Lukas[‡], and Yongchang Chang[‡2]

From the [‡]Division of Neurobiology, Barrow Neurological Institute and St. Joseph's Hospital and Medical Center, Phoenix, Arizona 85013, the [§]Department of Obstetrics and Gynecology, St. Joseph's Hospital and Medical Center, Phoenix, Arizona 85013, and the [¶]Department of Medical Genetics and Cell Biology, Guangzhou Medical College, Guangzhou 510182, China

Binding of a neurotransmitter to its membrane receptor opens an integral ion conducting pore. However, prolonged exposure to the neurotransmitter drives the receptor to a refractory state termed desensitization, which plays an important role in shaping synaptic transmission. Despite intensive research in the past, the structural mechanism of desensitization is still elusive. Using mutagenesis and voltage clamp in an oocyte expression system, we provide several lines of evidence supporting a novel hypothesis that uncoupling between binding and gating machinery is the underlying mechanism for α7 nicotinic receptor (nAChR) desensitization. First, the decrease in gate tightness was highly correlated to the reduced desensitization. Second, nonfunctional mutants in three important coupling loops (loop 2, loop 7, and the M2-M3 linker) could be rescued by a gating mutant. Furthermore, the decrease in coupling strength in these rescued coupling loop mutants reversed the gating effect on desensitization. Finally, coupling between M1 and hinge region of the M2-M3 linker also influenced the receptor desensitization. Thus, the uncoupling between N-terminal domain and transmembrane domain, governed by the balance of coupling strength and gate tightness, underlies the mechanism of desensitization for the α7 nAChR.

The Cys-loop receptor family of ligand-gated ion channels are allosteric proteins (1–4). Binding of neurotransmitter to the receptor binding site located in the N-terminal domain induces conformational changes (5), which propagate to the transmembrane domain (M1–M4)[3] through the interface between these two domains to open the gate, which is formed by M2 domains (see Fig. 1*A*). Coupling through this interface is mainly mediated by noncovalent interactions between loops 2 and 7 (Cys-loop) from N-terminal domain and M2-M3 linker from the transmembrane domain (see Fig. 1*B*) (6, 7). In addition, pre-M1 and M1 is the only covalent linkage between N-terminal domain and transmembrane domain, which also play a role in controlling channel gating (7). However, agonist binding does not guarantee channel opening. With prolonged exposure to neurotransmitters, most receptors are driven to a refractory state, termed desensitization (8). At the single channel level, desensitization appears as long-lasting nonconducting states (9). Desensitization is a widespread phenomenon in most ligand-gated ion channels. It plays an important role in shaping synaptic transmission (10, 11). Desensitization of the Cys-loop receptor family has been well characterized kinetically. It involves dramatic increase in binding affinity to agonists (12, 13) and closure of the ion conducting pathway (9) with little structural change in transmembrane domain (14). It is an intrinsic property of the receptors (15).

Previous studies have identified numerous factors that can influence desensitization. For example, desensitization is dependent on agonists (16) and receptor subtypes (17, 18). Mutations of a residue in the binding pocket (19) or between two binding loops (20) influence desensitization. A study using chimeric nAChR subunits suggests that two segments in the N-terminal domain are involved in desensitization (21). Another study using serotonin receptor type 3 ($5HT_3R$) chimeric with α7 nAChR fragments suggests that the interface between N-terminal domain and transmembrane domain, especially pre-M1 and the M2-M3 linker, is an important determinant for desensitization (22). In addition, mutations of a pre-M4 residue in the intracellular loop can alter desensitization (23). The most dramatic influences on desensitization kinetics are from the mutations in the pore-lining domain (M2). For example, introducing an aromatic residue to the M2 enhances desensitization (24–27), whereas substituting hydrophobic residues with hydrophilic ones markedly slows desensitization (25, 28) or even converts the fast desensitizing α7 nAChR to nondesensitizing (28). However, despite intensive studies in the past, the molecular mechanism for desensitization of the Cys-loop receptors is still poorly understood. There is no single mechanism that can explain most observations.

In this study, we proposed a novel hypothesis that uncoupling of N-terminal domain and transmembrane domain is a major mechanism for receptor desensitization, and this uncoupling is mainly determined by the balance of coupling strength (between loop 2/loop 7/M1 and M2-M3 linker) and gate tight-

* This work was supported by the NIGMS, National Institutes of Health Grant R01GM085237. This work was also supported by Arizona Biological Research Commission Grant ABRC0702 and the Barrow Neurological Foundation (to Y. C.) and in part by a St. Joseph's Foundation startup fund (to Y. H.).

[1] Present address: Beijing Institute for Neuroscience, Capital Medical University, Beijing Center of Neural Regeneration and Repair, Key Laboratory for Neurodegenerative Disease of the Ministry of Education, Beijing 100069, China.

[2] To whom correspondence should be addressed: Div. of Neurobiology, Barrow Neurological Institute, 350 W. Thomas Rd., Phoenix, AZ 85013. Tel.: 602-406-6192; Fax: 602-406-4172; E-mail: yongchang.chang@chw.edu.

[3] The abbreviations used are: M1-M4, transmembrane domains 1–4; nAChR, nicotinic acetylcholine receptor; α-BTX, α-bungarotoxin; $5HT_3R$, serotonin receptor type 3.

ness. We designed a series of experiments to test our hypothesis using fast desensitizing α7 nAChR expressed in *Xenopus* oocytes. First, we altered gate tightness by mutating the putative gating machinery to confirm and extend previous findings of the gating effect on desensitization. Second, with double mutations in coupling and gating regions, we observed the mutual interaction between these two regions and their effects on desensitization and channel gating. Finally, we defined the residues that couple the M1 and the hinge region of M2-M3 linker responsible for desensitization.

EXPERIMENTAL PROCEDURES

Mutagenesis and cRNA Preparation—The cDNA encoding the wild type human α7 nAChR subunit was cloned into the pGEMHE vector with T7 orientation. The residues in the loops 2 and 7 of the N-terminal domain, pre-M1 region, M2-M3 linker, and second transmembrane domain (see Fig. 1) were mutated to cysteine or other residues, both for single and multiple mutations, using the PCR-based QuikChange method of site-directed mutagenesis with *PfuUltra* DNA polymerase (Agilent Technologies, Hercules, CA). The mutations were confirmed by automated DNA sequencing (DNA laboratory, Arizona State University, Tempe, AZ). The wild type and mutant cDNAs were then linearized by NheI digestion. The cRNAs were transcribed by T7 RNA polymerase (New England Biolabs) using standard *in vitro* transcription protocols. After digestion of the DNA template by RNase-free DNase I, the cRNAs were purified and resuspended in diethyl pyrocarbonate-treated water. cRNA yield and integrity were examined on a 1% agarose gel (29).

Oocyte Preparation and Injection—Oocytes were harvested from female *Xenopus laevis* (*Xenopus* I, Ann Arbor, MI) as described previously (30) in accordance with the Institutional Animal Care and Use Committee-approved protocol of *Xenopus* care and use. The stage VI oocytes were selected and incubated at 16 °C before injection. Micropipettes for injection were pulled from borosilicate glass (Drummond Scientific, Broomall, PA) on a Sutter P87 horizontal puller, and the tips were cut with forceps to ≈40 μm in diameter. The cRNA was drawn up into the micropipette and injected into oocytes with a Nanoject micro-injection system (Drummond Scientific) with a total volume of 20∼60 nl.

Two-electrode Voltage Clamp—One to three days after injection, an oocyte expressing α7 nAChR was placed in a homemade small volume chamber with continuous perfusion with calcium free oocyte Ringer's solution 2, which consisted of the following: 92.5 mM NaCl, 2.5 mM KCl, 1.8 mM $BaCl_2$, and 5 mM HEPES, pH 7.5, to minimize activation of calcium sensitive chloride channels in oocytes due to high calcium permeability of the α7 nAChR. The oocyte Ringer's solution 2 also contained 1 μM atropine to avoid activation of muscarinic receptor in the oocytes. The chamber was grounded through an agar salt bridge to avoid the drug influence on junction potential between the grounding silver wire and solution. The oocytes were voltage clamped at −60 mV to measure acetylcholine-induced currents using a GeneClamp 500B two-electrode voltage-clamp amplifier (Axon Instruments, Foster City, CA). The current signal was low pass-filtered at 50 Hz with the built-in four-pole low pass Bessel filter in the GeneClamp 500B two-electrode voltage-clamp amplifier and digitized at 100 Hz with a Digidata1440a digitizer and pClamp 10 software (Axon Instruments).

Single Oocyte Binding—Four days after RNA injection, the control or α7 nAChR-expressing oocytes (follicular membrane-free) were individually placed in a low binding 96-well plate with a V-shaped bottom. The oocytes were individually incubated in 15 μl of 2 nM ^{125}I-labeled α-bungarotoxin (^{125}I-α-BTX, PerkinElmer Life Sciences) in oocyte Ringer's solution 2 with 1% BSA in each well at room temperature for 2 h. Each oocyte was then rinsed four times with 200 μl oocyte Ringer's solution 2 with BSA with a 10-min incubation at room temperature for each rinse. The oocytes were then transferred into a 96-well scintillation counting plate (one oocyte per well). After removing excess fluid, the oocytes were dissolved in 10 μl 0.01 M NaOH, 0.1% SDS solution per well. The dissolved individual oocytes were further disbursed in 200 μl scintillation fluid overnight before scintillation counting (1 min per well) with a 1450 MicroBeta TriLux Scintillation and Luminescence counter (PerkinElmer Life Sciences).

Drug Preparation—Acetylcholine chloride (ACh, Sigma-Aldrich) stock solution was prepared daily from the solid. Mecamylamine hydrochloride (Tocris, Ellisville, MO) stock solution was prepared and stored at −20 °C in aliquots before use.

Data Analysis—The dose-response relationship of the ACh-induced current in recombinant α7 nAChRs was least-squares fit to a Hill equation with Prism (version 4.0, GraphPad Software, Inc., San Diego, CA) to derive EC_{50} (the concentration required for inducing a half-maximal current), Hill coefficient (the slope factor), and maximum current. The maximum current was then used to normalize the dose response curve for each individual oocyte. The average of the normalized currents for each ACh concentration was used to plot the data. Statistical significance of the differences between wild type and mutant log(EC_{50}) values or between ^{125}I-α-BTX binding groups was determined by analysis of variance with post hoc Dunnett's test, or Tukey's multiple comparison test. Linear regression analysis was used to determine significance of correlation between two parameters. All data were presented as mean ± S.E.. Each group of data were confirmed in at least three oocytes. Coupling energy ($\Delta\Delta G$) was determined by mutant cycle analysis with the following equation: $\Delta\Delta G = RT\ln(\Omega)$, where R is gas constant, T is absolute temperature, and Ω is coupling coefficient ($\Omega = (EC_{50wt.wt} \times EC_{50mut1.mut2})/(EC_{50mut1.wt} \times EC_{50wt.mut2})$) (6, 31).

Homology Modeling—A three-dimensional model of the α7 nicotinic receptor subunit was made using Discovery Studio software (version 1.7, Accelrys, San Diego, CA) running in a Dell Precision 690 computer (Austin, TX). A single subunit was modeled as the following. Briefly, the human α7 nicotinic receptor subunit (1–303 and 413–480) were aligned to the corresponding region of the α subunit sequence of the *Torpedo* nAChR (chain A) from the Protein Data Bank code 2BG9 with modeler 9.0 in Discovery Studio software using "Align Sequence with Structure" protocol with the blosum62 scoring matrix, gap open penalty of −200, gap extension penalty of

−10, and default two-dimensional gap weights. The homology model was then built using "Building Homology Models" protocol without optimization and loop refinement, and with predefined disulfide bridges in the cysteine loops and double cysteines in the binding loop C. The model was further energy minimized for 400 steps of steepest descent minimization method followed by 1000 steps of conjugated gradient using minimization protocol with CHARMm force field. Structural model presentations shown in Fig. 1 were generated with Swiss-PdbViewer (version 4.0) and POV-ray software (version 3.6) for Windows.

RESULTS

Weakening Hydrophobic Interaction of Gating Residues Shifted Dose-response Curve to Left and Reduced Receptor Desensitization—The coupling between N-terminal domain and channel-lining domain is mainly through noncovalent interactions (6, 32–34). The gating machinery is also formed by noncovalent interactions (34–36). Thus, tightness of the gate relative to the coupling strength would influence the coupling efficiency to transduce binding energy to the gating machinery. Previous studies have demonstrated that mutations of the hydrophobic gate-forming residues to hydrophilic ones significantly increase receptor sensitivity to agonist (37) and decrease desensitization (25, 28). In extreme cases, these pore mutants produce nondesensitizing receptors (28). To reproduce this effect and further expand the covering region of the gating machinery, we scanned the M2 region at 7′–19′ positions (Val^{246}–Ala^{258}) with hydrophilic serine mutations. (The M2 positions are numbered from intracellular end starting with Ile^{240} as 1′.) The EC_{50} values of these mutants are listed in Table 1. Fig. 2*A* demonstrates that hydrophilic mutations of the four M2 residues resulted in a dramatic (>10-fold) leftward shift of the dose-response curve when compared with that for the wild type receptor. These four residues are highlighted in Fig. 1*C*. The largest shift was produced by the mutation at 13′ position (V252S), followed by 9′ position (L248S), and then 17′ (L256S) and 16′ (L255S) positions. At the same time, the spontaneous current in the absence of agonist was also evident in some mutants. These currents were blocked by mecamylamine, the noncompetitive antagonist of the α7 nAChR (Fig. 2*B*). For an allosterically activated receptor, higher sensitivity to agonist and spontaneously openings of hydrophilic mutants suggest that the mutations at these positions have lowered the gating energy, and the gating machinery is determined by the hydrophobic interactions mainly at 9′ and 13′ positions and, to a lesser extent, at 16′ and 17′ positions. Fig. 2*C* shows typical traces from these mutants by a saturation concentration of ACh. Compared with the wild type, all four mutants exhibited a marked decrease in desensitization. Fig. 2*D* plots

TABLE 1
EC_{50} values of ACh-induced currents in the M2 mutants of α7 nAChR

Mutants	Current			
	EC_{50}	Fold change in EC_{50}	n_H	n
	μM			
V246S	72.66 ± 7.78[a]	−3	1.28 ± 0.09	6
L247S	nonfunctional			
L248S (9′)	0.43 ± 0.01[a]	−490	3.07 ± 0.09	3
S249S (WT)	210.52 ± 24.29	1	1.01 ± 0.06	6
L250S	98.67 ± 10.82[a]	−2	2.17 ± 0.27	5
T251S	114.14 ± 8.68[b]	−2	2.60 ± 0.30	5
V252S (13′)	0.32 ± 0.01[a]	−658	1.14 ± 0.14	3
F253S	157.87 ± 12.72	1	1.03 ± 0.01	6
M254S	154.18 ± 8.04	1	1.43 ± 0.14	6
L255S (16′)	7.76 ± 0.14[a]	−27	2.66 ± 0.12	4
L256S (17′)	3.47 ± 0.16[a]	−61	2.09 ± 0.24	6
V257S	30.72 ± 2.00[a]	−7	1.07 ± 0.09	6
A258S	266.30 ± 33.71	1	1.15 ± 0.04	5

[a] $p < 0.001$ compared with wild type.
[b] $p < 0.01$.

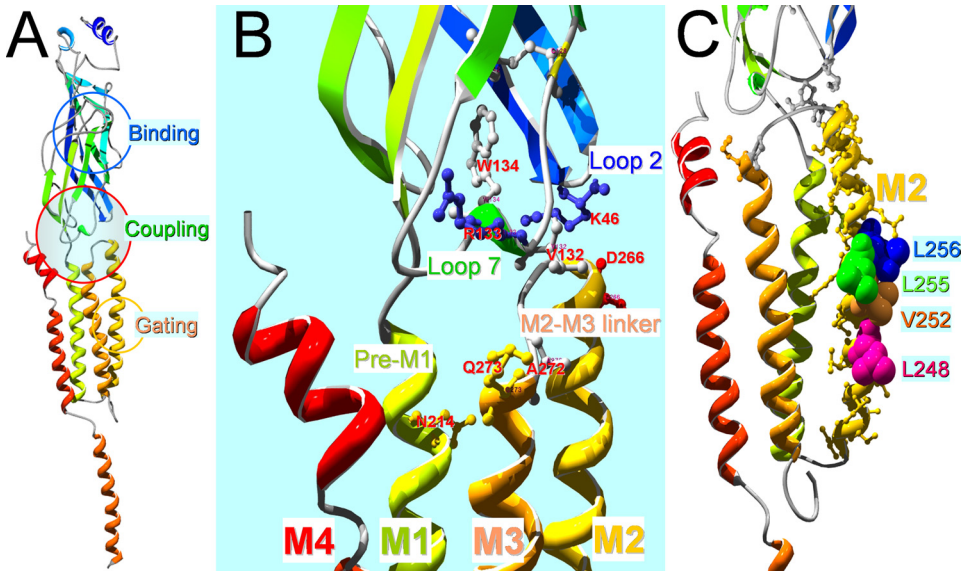

FIGURE 1. **Homology model of the human α7 nAChR subunit.** *A*, overall structure of a single subunit with a large part of the major intracellular loop missing as original 4 Å EM structural template (Protein Data Bank code 2BG9) of the α subunit of the *Torpedo* nicotinic receptor. Note that there are three important functional domains in each subunit. The binding domain is located in the middle of the N terminus. The gating machinery is in the transmembrane domain, mainly formed by 5-s transmembrane domains (*M2s*), one from each subunit. The coupling region between the two domains is formed by multiple loops as detailed in *B*. *B*, a closer look of the coupling region, which is mainly contributed by loop 2 and loop 7 from the N-terminal domain and M2-M3 linker from the transmembrane domain. Pre-M1 and the extracellular end of M1 are also in close proximity of the M3 side of the M2-M3 domain from a neighboring subunit (not shown). The labeled residues are important coupling residues used in this study. *C*, a closer look of the M2 domain with the gating residues labeled.

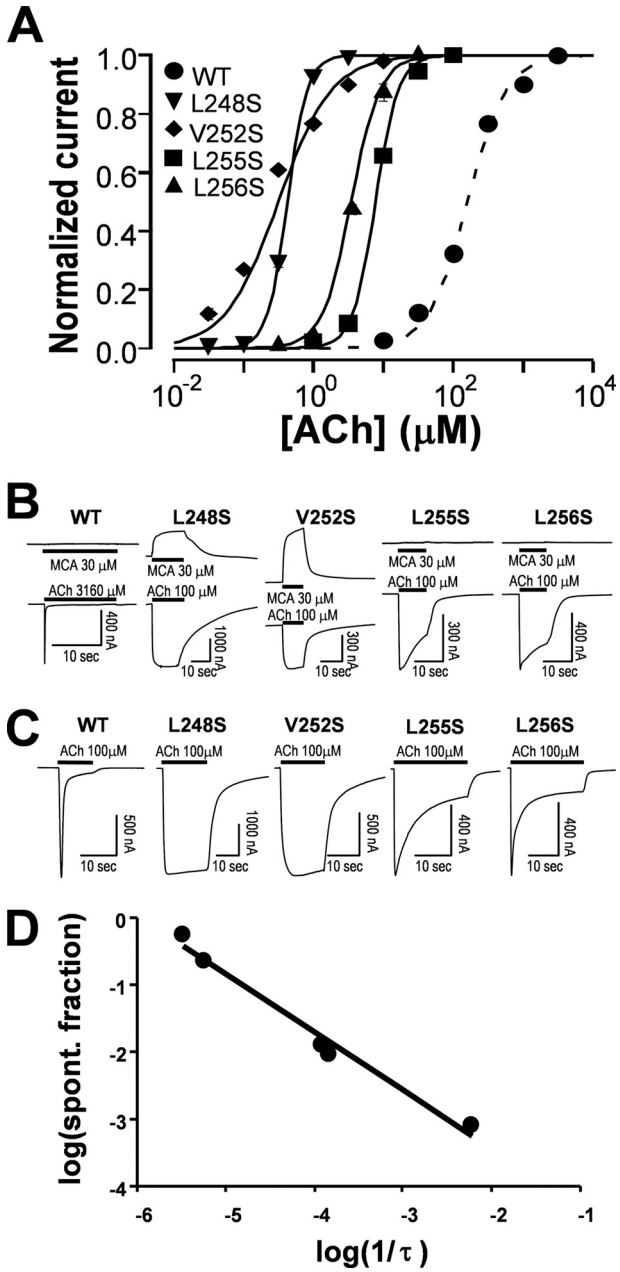

FIGURE 2. **Relationship of gating and desensitization.** *A*, normalized and averaged dose-response relationships for four mutants with significant shift of the dose-response relationship when compared with the wild type receptor. EC_{50} values for these mutants, along with other mutants, are listed in Table 1. *Error bars* are smaller than the symbols. Note that compared with the wild type receptor, all four M2 mutants exhibited higher sensitivity to ACh. *B*, spontaneous currents were evident when they were blocked by nAChR antagonist mecamylamine (*MCA*). The maximal activatable currents were determined by a saturation concentration of ACh. *C*, the rate of desensitization was slower in four gating mutants when compared with that for the wild type receptor. *D*, the desensitization rate and fraction of spontaneous (*spont.*) opening (spontaneous current/total current (spontaneous + activatable)) were highly correlated ($p = 0.001$; $r^2 = 0.9818$).

the relationship between desensitization rate and fraction of spontaneous current. Interestingly, the desensitization rate was negatively correlated to the fraction of spontaneous current in log scale. Thus, the extent of the gating energy reduction, reflected by the fraction of spontaneous current (see "Discussion" for details), was correlated to the degree of reduced desensitization.

Mutation of Putative Coupling Residues in Loop 2 Disrupted Channel Function, Which Was Rescued by Gating Mutant—In the *Torpedo* nAChR α subunit, the coupling between binding and gating domains is proposed to be mediated by the hydrophobic interaction between Val^{44} in loop 2 and Ser^{269}–Pro^{272} in the M2-M3 linker (34). The homologous residue of Val^{44} in α7 nAChR is a positively charged residue, Lys^{46}. In our homology model (Fig. 1*B*), this residue is close to the negatively charged residue of Asp^{266} in the M2-M3 linker. Thus, the coupling of binding and channel gating in α7 nAChR could be mediated by a charge interaction. To test this hypothesis, we made multiple mutations at these two residues. Mutations of Lys^{46} to Trp, Phe, Cys, Asp, and Asn, and mutations of Asp^{266} to Cys, Leu, and Gln resulted in nonfunctional channels (data not shown), suggesting the importance of both residues in channel function. However, K46A, K46Q, and D266A mutants were functional with no discernable changes in desensitization kinetics (data not shown). With some functional mutants, we further performed mutant cycle analysis by measuring EC_{50} values for WT (210.52 ± 24.29 μM, $n = 6$), K46R (239.53 ± 23.03 μM, $n = 3$), D266E (355.37 ± 30.60 μM, $n = 3$), and K46A/D266A (810.90 ± 97.87 μM, $n = 3$). The resulting coupling energy calculated from above values indicated that there is only a very weak coupling ($\Delta\Delta G = 0.41$ kcal) between these two residues, consistent with the unified view of coupling mechanism in the Cys-loop receptor family (38) and the conclusion of unlikely pairwise interaction of these putative coupling residues in the α7 nAChR (39).

To further test the hypothesis that relative strength of coupling and gating energy govern the ultimate outcome of channel gating, we constructed double mutants with one nonfunctional loop 2 mutation and one gating mutation. The result revealed that several nonfunctional mutants of Lys^{46} (K46C, K46D, and K46N) were rescued by a gating mutant V252S (Fig. 3, *A* and *B*, with K46D and K46N shown). Notably, when compared with gating mutant V252S alone, the rescued double mutants also exhibited a rightward shift of the dose-response curve (Fig. 3*C*) and an increase in desensitization rate (Fig. 3*D*). Thus, weakening the coupling strength can increase receptor desensitization, (in the extreme case, such as nonfunctional mutants, the agonist binding probably directly drives the receptor into the desensitized state without activating it), whereas reducing the gate tightness can counteract that effect.

Nonfunctional Mutant of Loop 7 Coupling Residues Was Rescued by Gating Mutant—In addition to loop 2, several studies have demonstrated that loop 7 (Cys-loop) is also important in coupling between N-terminal domain and gating machinery in α7 nAChRs (39), $GABA_A$ receptor (6, 33), or ACh binding protein coupled to the C-terminal domain $5HT_3R$ (32). To demonstrate similar importance of the balance between coupling strength through loop 7 and gating energy in channel activation and desensitization, we generated a mutant in several previously identified important coupling residues (V132I/R133Y/W134N) in loop 7. Mutations of these residues totally impaired channel functions (data not shown). However, with the combination of a gating mutation (V132I/R133Y/W134N/V252S), the receptor became functional (Fig. 4*A*). Because weakening of coupling strength would decrease channel gating efficiency, rightward shifts of EC_{50} values for gating mutants by the cou-

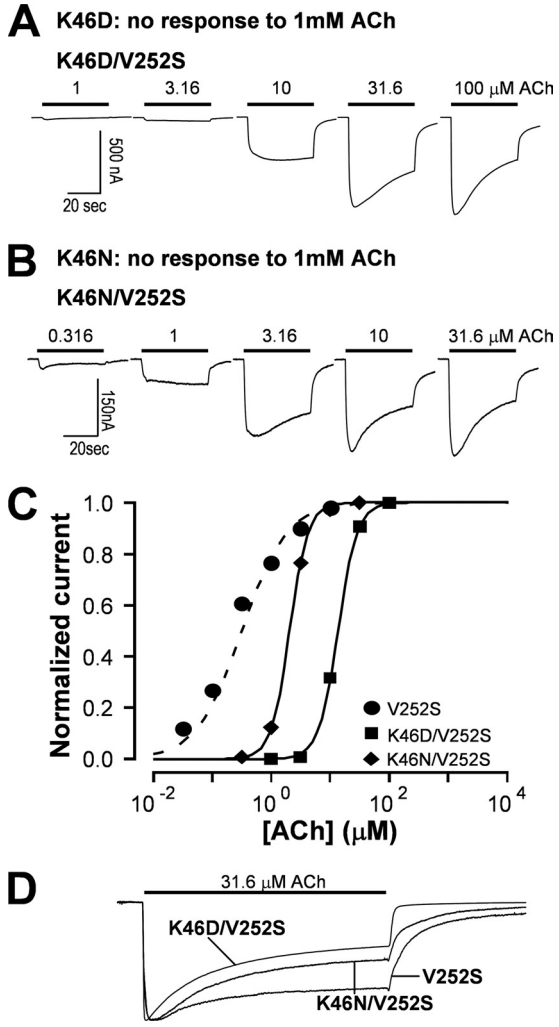

FIGURE 3. **Nonfunctional loop 2 mutants were rescued by a gating mutation with altered desensitization kinetics compared with the gating mutant alone.** *A*, the K46N mutant was not functional. However, addition of V252S mutation to the K46N mutant rescued the function of the receptor. *B*, the K46D mutant was not functional. However, addition of V252S mutation rescued the function of the receptor. *C*, the ACh dose-response relationships of the rescued receptors exhibited rightward shift (EC_{50} = 13.40 ± 0.32 μM for K46D/V252S and EC_{50} = 2.04 ± 0.05 μM for K46N/V252S) when compared with that for the V252S mutant alone (EC_{50} = 0.32 ± 0.01 μM). *Error bars* are smaller than the symbols. *D*, the rescued mutant receptors also had faster desensitization kinetics when compared with the gating mutant alone (τ_{V252S} = 15.60 ± 0.58 s, $n = 4$; $\tau_{V252S/K46N}$ = 13.92 ± 0.21 s, $n = 4$, $p < 0.05$; $\tau_{V252S/K46D}$ = 12.95 ± 0.49 s, $n = 3$, $p < 0.05$).

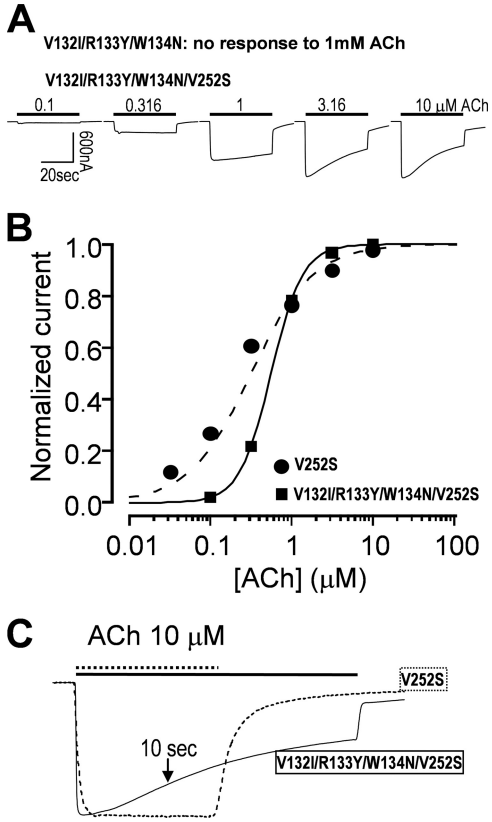

FIGURE 4. **A nonfunctional loop 7 mutant (V132I/R133Y/W134N) could be rescued by a gating mutation with altered desensitization kinetics compared with the gating mutant alone.** *A*, the V132I/R133Y/W134N mutant was not functional. However, addition of V252S mutation to the mutant rescued the function of the receptor. *B*, the ACh dose-response relationships of the rescued receptor (V132I/R133Y/W134N/V252S) exhibited rightward shift (EC_{50} = 0.56 ± 0.02 μM) when compared with V252S alone. *Error bars* are smaller than the symbols. *C*, the rescued receptor had faster desensitization kinetics when compared with the gating mutant alone (fraction of remaining current relative to the peak after 10-s ACh application was 0.75 ± 0.01 for the rescued receptor (V132I/R133Y/W134N/V252S) and 0.98 ± 0.01 for V252S mutant alone; $p < 0.001$). Note that due to limited desensitization of the 10 μM ACh-induced current in V252S, exponential fitting for time constant was not successful.

pling mutants were expected and experimentally confirmed (Fig. 4*B*). At the same time, incorporation of nonfunctional coupling mutants also significantly increased desensitization of the gating mutant (Fig. 4*C*). Although we did not dissect individual contributions of these loop 7 coupling residues, the above observation has already served for its purpose in supporting the notion that the balance between coupling strength and gate tightness in determining desensitization kinetics is not limited to loop 2 but also applicable to loop 7.

Nonfunctional Mutant D266C of M2-M3 Linker Was Rescued by Gating Mutant—Thus far, we have tested two important coupling loop mutants in the N-terminal domain for their roles in receptor desensitization. Because the M2-M3 linker from the transmembrane domain is also a key structural component of coupling, here, we further tested whether the reduction of hydrophobic interaction at the channel gate could also rescue nonfunctional mutants in this region. Asp^{266} has been identified as a crucial coupling residue in the M2-M3 linker (40). Thus, we tested the effect of a mutation of this residue on channel function and desensitization. Our result demonstrated that the D266C mutant was not functional (data not shown). However, when we added a gating mutation (V252S), the double mutant receptor (D266C/V252S) became functional (Fig. 5*A*). The dose-response curve of the V252S mutant was shifted to the right when the D266C mutation was introduced into the channel (Fig. 5*B*). Concomitantly, desensitization kinetics also speeded up for the same agonist concentration when compared with V252S single mutant (Fig. 5*C*).

In above experiments, we used loss-of-function mutants in the coupling region to demonstrate that the balance between coupling strength and gating tightness govern the receptor gating and desensitization. Because there are no tightly coupled residue pairs in the coupling region identified, it is not easy to use cross-linking to strengthen coupling for the gain-of-func-

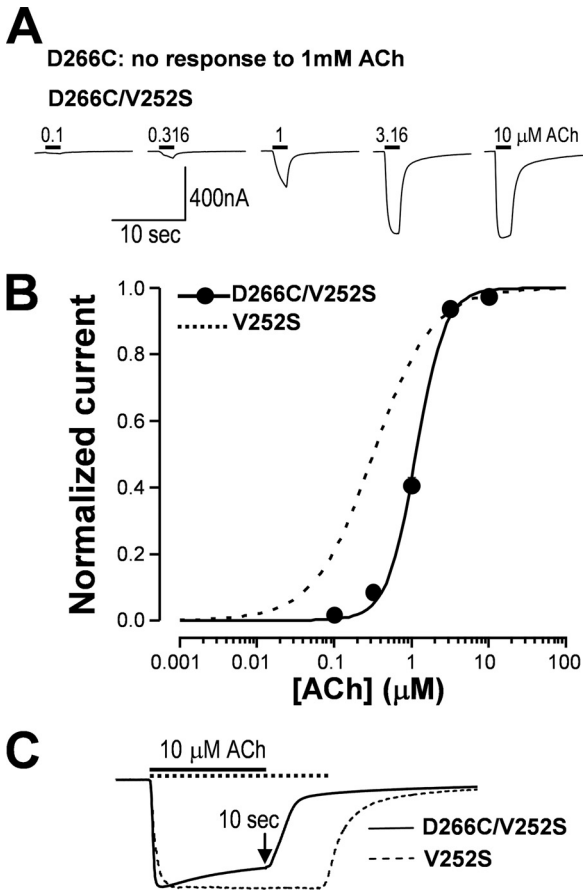

FIGURE 5. **A nonfunctional mutant (D266C) in the M2-M3 linker could be rescued by a gating mutation with altered desensitization kinetics compared with the gating mutant alone.** *A*, the D266C mutant was not functional. However, addition of V252S mutation to the mutant rescued the function of the receptor. *B*, the rescued receptors (D266C/V252S) exhibited rightward shift of the ACh dose-response relationship ($EC_{50} = 1.15 \pm 0.05$ μM) when compared with the V252S mutant. *C*, the rescued receptor had faster desensitization kinetics when compared with the gating mutant alone; the fraction of remaining current relative to the peak after a 10-s ACh application was 0.81 ± 0.03 for the rescued receptor and 0.98 ± 0.01 for V252S alone ($p < 0.01$).

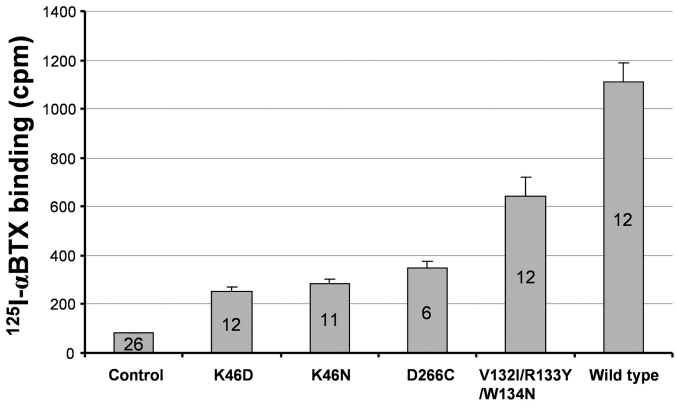

	Control	K46D	K46N	D266C	V132I/R133Y/W134N	Wild type
Control						
K46D	P<0.05					
K46N	P < 0.01	P > 0.05				
D266C	P < 0.01	P > 0.05	P > 0.05			
V132I/R133Y/W134N	P < 0.001	P < 0.001	P < 0.001	P < 0.01		
Wild type	P < 0.001	P < 0.001	P < 0.001	P < 0.001	P < 0.001	

FIGURE 6. **Nonfunctional mutant receptors, used in the rescuing experiments in Figs. 3–5, exhibited ^{125}I-α-BTX binding above the background.** The bar graph represents the average ^{125}I-α-BTX bindings in the mutant and wild type receptor-expressing single oocytes or nonexpressing controls. Number of oocytes used in the binding experiments in each group is indicated in each *bar*. The *p* values for analysis of variance post hoc multiple comparison tests are shown *below* the bar graph. Note that the binding in the control oocytes represents nonspecific binding, and all mutant and wild type receptor-expressing oocytes exhibited higher-than-background binding, suggesting that all these mutant receptors have some level of surface expression. Note that all the mutant-expressing oocytes had lower binding values compared with the wild type-expressing oocytes, although with a similar amount of cRNA injection. After subtracting background control value, their specific bindings are 16.5% (K46D), 19.7% (K46N), 25.9% (D266C), and 54.3% (V132I/R133Y/W134N) of the wild type binding.

tion influence on receptor desensitization. In fact, our attempt using an oxidation agent in several double cysteine mutants such as K46C/D266C and several pairs of adjacent residues between loop 2 and M2-M3 linker failed to produce functional channels. This precluded us from further pursuing the cross-linking study in the coupling region. (Note that reducing agents can break disulfide bonds in the binding loop C and make channels nonfunctional.) Nevertheless, our data are strong enough to support our hypothesis.

To exclude the possibility that non-functional mutants used in above rescue experiments were due to complete absence of the mutant receptors in the plasma membrane, we performed ^{125}I-α-BTX binding assay for oocytes expressing mutant or wild type receptors compared with the non-expressing control. Fig. 6 shows that these mutant receptors exhibited significantly higher ^{125}I-α-BTX binding than the control. Thus, these nonfunctional mutants all have surface expression, although the level of binding of these mutants was reduced when compared with that for the wild type receptor. Lower binding of the mutant receptors is likely due to different batches of the cRNAs synthesized using different batches of the RNA CAP structure. When we measured binding using the oocytes injected with new cRNAs, the ^{125}I-α-BTX binding of mutant receptors is indistinguishable from the wild type receptor (data not shown). The extent of the reduced binding in Fig. 6, however, cannot explain total loss of function in these mutants, further suggesting that complete uncoupling is mainly responsible for the total loss of function in these mutants.

Coupling between M1 and M2-M3 Linker Also Influences Desensitization Kinetics—A study of 5-HT_3R with the chimeric incorporation of α7 nAChR segments also pointed out another important mechanism for channel gating and desensitization (22). That study demonstrated that the pre-M1 and beginning of M1 can interact with the end of M2-M3 linker, and such an interaction determines channel activation and desensitization kinetics. However, the underlying interacting residues have not been determined yet. It is also not clear whether the similar coupling between M1 and M2-M3 linker is also an important gating determinant in the α7 receptor-based chimera. To identify important residues in this potential coupling region in α7 nAChR, we scanned the M2-M3 linker (Asp^{266} to Tyr^{274}) with cysteine mutagenesis. Our results indicated that majority of mutants either were nonfunctional (*e.g.* D266C and S267C) or had very low expression levels (*e.g.* P269C, L270C, I271C, and Y274C), suggesting that residues at these positions are important in channel function. The V268C mutant was functional but with strong desensitization (data not shown). However, two mutants, A272C and Q273C, exhibited slowed desensitization kinetics (Fig. 7*A*). Interestingly, α7A272 is homologous to the

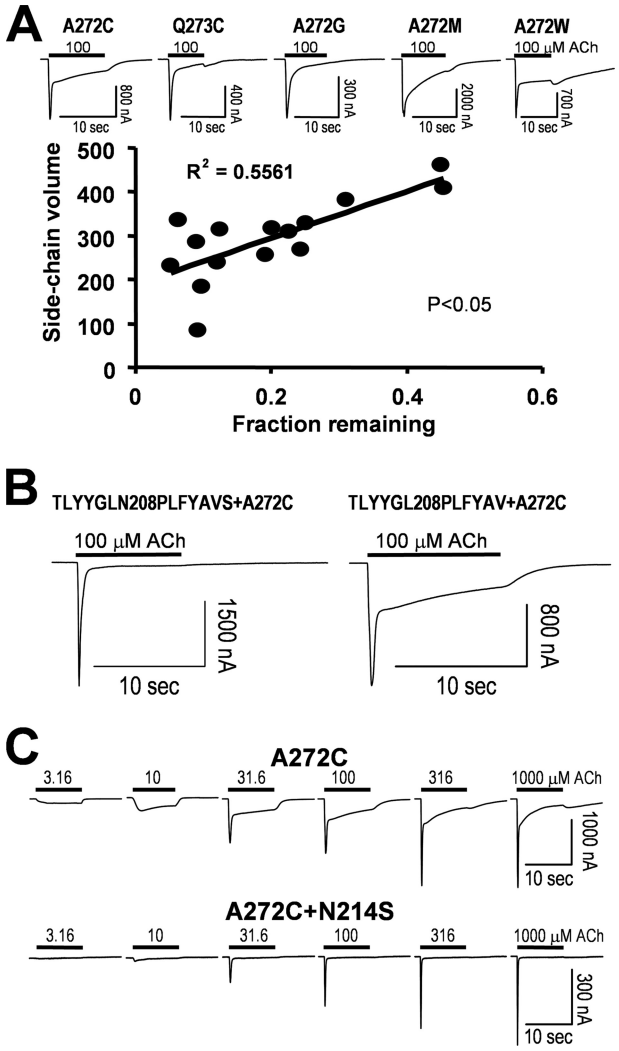

FIGURE 7. **Interaction between M1 and the M2-M3 linker altered the α7 nAChR desensitization.** *A*, M2-M3 linker mutagenesis scanning resulted identification of two positions that can slow the channel kinetics upon mutations (with sample current traces of several mutants). Note that some mutants such as A272C exhibited double exponential decay, and in others, such as A272W, agonist block was evident (with a hump current after switching to control solution). Thus, in correlation analysis, we use fraction remaining at 10 s of ACh application, instead of time constant of current decay. *B*, a seven-residue (208–214) substitution in pre-M1 abolished the slow component of A272C mutation, whereas a six-residue (208–213) substitution (without mutation at Asn^{214}) had no effect on the current kinetics. *C*, N214S/A272C double mutants further confirmed that Asn^{214} interacting with A272C is an important determinant for desensitization.

putative hinge residue of α1Gly^{275} in the *Torpedo* nAChR (34). To address whether the slowed desensitization is due to an increase in side chain size and thus a decrease in hinge flexibility, we performed all possible substitutions of this putative hinge residue (Ala^{272}). Three mutants (A272K, A272R, and A272P) were nonfunctional (data not shown). The remaining functional mutants showed different degrees of desensitization. Because some mutants exhibited a double exponential decay, we used the fraction of the remaining current after decaying from the peak as a parameter. Note that the fraction of the remaining current after a 10-s application of 100 μM ACh was positively correlated to the side chain volume (Fig. 7*A*, $p = 0.0113$) at position 272, suggesting that hinge hypothesis may play a role in the desensitization of α7 nAChR. That is, the more flexible the hinge, the faster desensitization kinetics for the receptor.

Alternatively, the size of side chain could influence coupling to other part of the receptor, and this coupling would contribute to its desensitization kinetics. As mentioned above, the interaction between M1 and the M2-M3 linker is an important determinant for receptor desensitization. We then replaced TLYYGLN sequence in the M1 region of α7 nAChR with the homologous sequence PLFYAVS from 5-HT_3R. When this chimera was added to the A272C mutant, the slowing effect on desensitization by A272C was abolished (Fig. 7*B*, *left panel*), suggesting coupling between Ala^{272} and the M1 segment is also important for the receptor desensitization. In contrast, when a shorter sequence of TLYYGL was replaced by PLFYAV, the chimera did not abolish the slowing effect of A272C on desensitization (Fig. 7*B*, *right panel*). Using this approach, we identified that Asn^{214} in M1 is an important residue for the receptor desensitization. In fact, with double mutation (N214S/A272C), N214S alone is enough to abolish the slowing effect of A272C on the receptor desensitization (Fig. 7*C*). Thus, the coupling between Asn^{214} and Ala^{272} mutants could influence receptor gating and desensitization. Coupling energy ($\Delta\Delta G = 0.97$ kcal) calculated from the EC_{50} values of the wild type (210.52 ± 24.29 μM, $n = 6$), N214S (97.37 ± 8.72 μM, $n = 3$), A272C (30.84 ± 0.67 μM, $n = 3$), and N214S/A272C (73.29 ± 2.97 μM, $n = 4$) mutants also suggests that these two residues, probably between two neighboring subunits, are coupled with intermediate coupling strength.

DISCUSSION

Despite intensive research in the past, the mechanism of desensitization of the Cys-loop receptors is still not completely clear. To this end, we provided several lines of evidence to support the hypothesis that uncoupling between loop 2/loop 7/M1 and M2-M3 is an important mechanism for desensitization, and this uncoupling is mainly governed by the balance between coupling strength and relative tightness of gating machinery. First, hydrophilic substitution of a gating residue dramatically reduced desensitization; and the change of desensitization was correlated to the extent of spontaneous current. Second, loss-of-function mutations of many putative coupling residues in loop 2, loop 7, and the M2-M3 linker were rescued by gating mutations. At the same time, the double mutants in the coupling and gating regions demonstrated the effect of mutual interaction of the two regions on desensitization kinetics. Finally, interaction between M1 and M2-M3 linker was also an important determinant for the receptor desensitization. Thus, strength of coupling energy relative to gating energy determines the likelihood of uncoupling and thus the extent of desensitization.

Our results and hypothesis can be best illustrated in Fig. 8 in terms of gating energy and coupling energy. When the bound agonist molecules induce conformational changes in the N-terminal domain to a high affinity state (flip state), the binding energy is then transmitted to the channel gate through the coupling region. The efficiency of this energy transduction from binding site to channel gate is probably dependent on the coupling strength relative to the gate tightness, which, in turn,

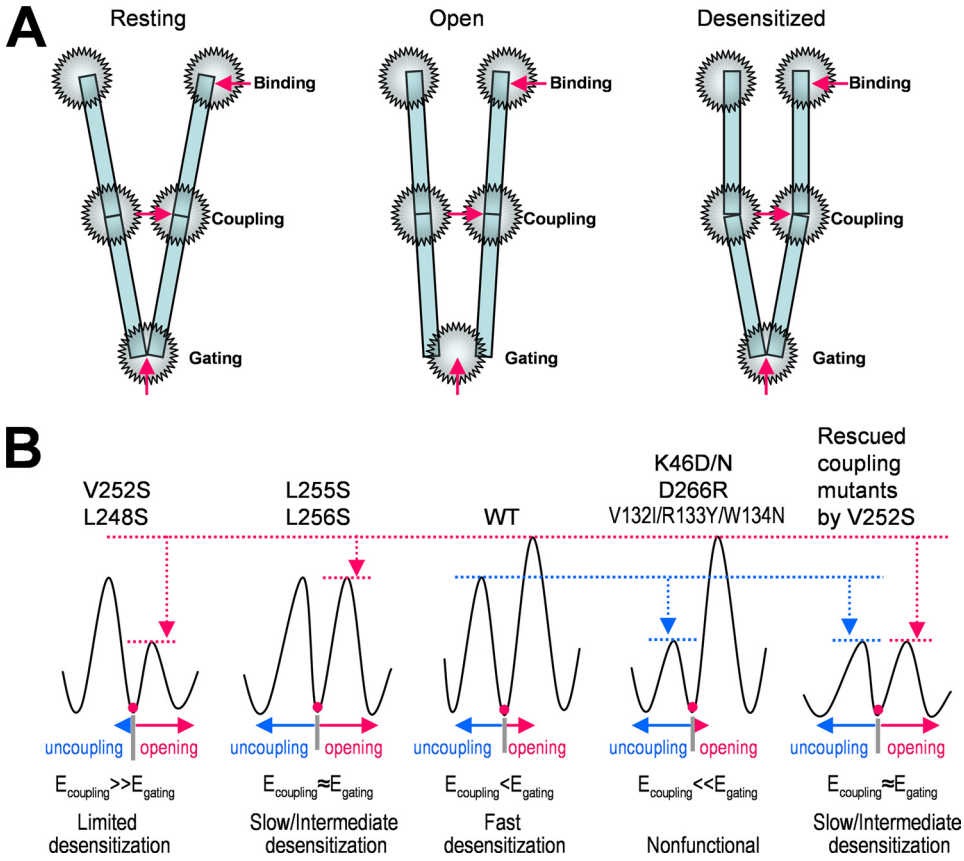

FIGURE 8. **Channel opening and desensitization is determined by the balance of binding, coupling, and gating regions.** *A*, a schematic presentation of three energetic hot spots for channel function: binding, coupling, and gating. In the resting state, the coupling region is intact, and the channel gate is closed (*left*). Upon agonist binding, the binding energy induces conformational changes of the receptor to overcome the gating energy barrier to open the channel through the stressed coupling region (*middle panel*). The stressed coupling region can break, which will cause uncoupling between binding site and channel gate. This uncoupling is desensitization (*right*). The likelihood of uncoupling depends on the relative strength of coupling and gating machinery as illustrated in *B*. *B*, putative energy profile in coupling and gating regions and their relationship to desensitization in the wild type and mutant receptors. E_{gating}, the energy needed to break the gating energy barrier to open the channel; $E_{coupling}$, energy needed to break the coupling energy barrier to desensitize the receptor. Thus, it is the relative strength of coupling energy and gating energy determine the degree and rate of desensitization.

determines the probability of the receptor going to a desensitized state. In wild type α7 nAChR, the coupling energy could be slightly lower than the gating energy, so that the receptor has fast desensitization. However, if the gating energy is markedly reduced, as in the cases of L248S and V252S, then the coupling energy is significantly higher than the gating energy. Under this condition, the uncoupling becomes unlikely, and desensitization is very limited. If the reduction of gating energy barrier is less dramatic, as in L255S and L256S mutants, the coupling energy could be similar to (or slightly higher than) the gating energy. In this case, the uncoupling is evident, and desensitization is intermediate. On the other hand, if the coupling strength is reduced dramatically, as in the cases of K46(D/N), D226C, and V132I/R133Y/W134N mutants, then the coupling energy is not enough to transduce binding energy to the gating machinery for channel opening. Under these conditions, the receptor is nonfunctional. In other words, upon agonist binding, all the receptors directly go to the desensitized state without activation. However, these nonfunctional mutants still have some subthreshold coupling strength for channel activation. Thus, when the energy barrier for activation was lowered with introduction of V252S mutation, the receptor becomes functional again, but with a slightly higher desensitization rate than the gating mutant alone.

Our hypothesis is not only consistent with our current findings but also can explain other M2 mutational effects on desensitization. For example, aromatic substitutions in the M2 domain (24, 25) would strengthen the hydrophobic interaction of the gating residues and thus increase tightness of the channel gate and enhance desensitization. Hydrophilic substitutions would weaken the energy barrier for channel opening, thus requiring less coupling energy and binding energy to open the channel and with reduced desensitization (25, 28). Although in this study, we focused on the balance of coupling and gating, our hypothesis does not exclude the possibility that other regions in the receptor subunits could impact desensitization. In most cases, we can interpret their effects on desensitization by indirect influence of coupling and gating.

Conducting Desensitized State—Hydrophilic mutation of the conserved M2 leucine L247T of the chicken α7 nAChR, which is homologous to L248T of the human α7 nAChR, created a high conductance state (80 ps). Based on this new conductance state, it has been proposed that the gating mutation created conducting desensitized state (28, 41). However, high conductance state is the only conducting state opened by low concentration of ACh or by its antagonists. Higher ACh concentration can induce openings with both normal conductance and high conductance. If the high conductance state is the desensitized

state, the opposite concentration dependence for the high conductance state should be expected because a higher concentration of agonist would induce more desensitization. In addition, the M2 9′ residue is not the only residue that forms the channel gate. At least three more residues at 13′ (34), 16′, and 17′ (this study) also form the energy barrier for channel gating. Furthermore, the major selectivity filter is located in the intracellular end of M2 (42). Interestingly, recent crystal structure studies of bacterial pentameric proton-gated ion channels (43, 44) suggest a M2-M3 tilting model for channel activation. In this model, M2-M3 tilting opens extracellular half of the pore and restricts the intracellular end of the pore for ionic selectivity and single channel conductance. Protonation scanning of M2 domain also supports the pore dilation mechanism in a nAChR (45). Thus, it is possible that L247T mutation decreases the gating energy barrier and creates an intermediate state with partial tilting of M2-M3, which opens the gate with less restriction in the intracellular end of the pore, resulting in a larger single channel conductance. In the wild type receptor, this partial tilting does not exist probably because higher energy barrier for channel gating prevents this partial conformational state.

Role of N-terminal Domain in Desensitization and Recovery—The molecular basis for faster desensitization of β2 subunit-containing nAChR than β4 subunit-containing nAChR lies in the N-terminal domain, mainly in two segments located in the top of the receptor (21). Although detailed residues underlying this difference have not been identified, it is clear that multiple residues in the N-terminal domain, with perhaps mutual interactions, are responsible for the different desensitization kinetics. How is this phenomenon related to uncoupling? One possibility is that interactions between the two segments in the β2 subunit create an energy trap in the N-terminal domain to increase binding affinity and to facilitate over-rotation in the N-terminal domain, resulting in extra stress on the coupling region. Thus, conformational change in the N-terminal domain can indirectly influence uncoupling of the binding and channel gate. The energy trap created by additional interactions is further supported by agonist-independent recovery of high affinity desensitization state. The subunit rearrangement in the N-terminal domain would bring some residues in the interacting range. For example, transient interactions between loop C and β7 (46) or between binding loops C and F (47) upon channel activation might also influence desensitization and recovery. In this sense, conformational changes in the N-terminal domain in both activation and desensitization could be very similar, but with different degrees.

Role of Intracellular Loop—The pre-M4 region of the M3-M4 intracellular loop is in close proximity to the selectivity filter formed by the pre-M2 and M2 domains. Hydrophobicity of mutants of a conserved arginine in $5HT_3R$ is positively correlated to the time constant of desensitization (23). This relationship is opposite to the effect of hydrophobicity of gating residues on the receptor desensitization. It is possible that channel opening causes restriction of intracellular end of the pore as suggested by two recent studies with bacterial proton-gated ion channels (43, 44). Narrowing of the intracellular end of the pore may also bring pre-M4 hydrophobic residues together to the range for their hydrophobic interaction. As a result, hydrophobic interaction between the intracellular residues could counteract the gating residues to stabilize receptor in the open state, reducing the gating energy and decreasing likelihood of uncoupling and desensitization.

Subunit-dependent Desensitization—The desensitization rate and level varies greatly with different members of this receptor family. Even within a subfamily, different subtypes of receptors also show dramatic difference in desensitization. For example, the desensitization rate among the heteromeric nAChRs are in the following order: $\alpha3\beta2 > \alpha4\beta2 > \alpha3\beta4 > \alpha4\beta4$ (18). The difference in desensitization among different subfamilies or subtypes could arise from variations in less important binding residues and in many important coupling residues. Even in the transmembrane domain, many residues are not absolutely conserved. Thus, variations in binding affinity, coupling strength, and gate tightness in different subunits can influence the uncoupling of binding and gating directly or indirectly. Because desensitization can help shape synaptic transmission (10), evolution must play a critical role in optimizing the receptor subunits for the receptor desensitization kinetics to match their functional role in synaptic transmission and extrasynaptic activity.

Desensitization without Activation—Activation of the Cys-loop receptor involves conformational change (flip state) in the binding site before channel gating (1, 48). In the case of a highly desensitizing channel, such as α7 nAChR, our data suggest that weak coupling strength relative to strong gate tightness makes it highly possible that uncoupling can occur before channel opening. In fact, cyclical desensitization model proposed more than 50 years ago has correctly predicted the possibility of desensitization without activation (8). In our data, the nonfunctional mutants in coupling region could be 100% desensitization without activation because of insufficient coupling energy for those mutant channels to open.

Two-gate Mechanism—It has been proposed that the nicotinic receptor has a desensitization gate in addition to the activation gate (49), similar to the "ball and chain" mechanism of the N-type inactivation of potassium channels, except that these two gates are mutually coupled. With this model, desensitization rate is much faster in the activated receptor than the resting receptor, and recovery from desensitization requires one more state with two discrete evens, *i.e.* opening of desensitization gate and closing activation gate, along with the changes in interaction between the two gates. The key point for the two-gate mechanism is that the activation gate is still in the open position after desensitization. A study using the cysteine accessibility test does not support an entirely separate desensitization gate or that the activation gate remains open in desensitized state (50). If the activation gate is closed in the desensitized state, then the two-gate model would be indistinguishable from the one-gate allosteric model with the uncoupling mechanism for desensitization as we proposed. In this case, in the open state, the tension sensed by the coupling loops is much higher than that in the resting state. Thus, the receptor is more likely to become uncoupled in the open state than in the closed state. In addition, when the M2 domain is uncoupled to the N-terminal domain, the conformation of this channel-lining domain does not necessarily need to be the same as in the rest-

ing state. Finally, recovery from desensitization clearly requires an extra step for recoupling. This would be equivalent to the reopening of the desensitization gate. In this sense, the coupling machinery can serve as the "desensitization gate," but working in a reversed manner.

In summary, we have proposed an uncoupling mechanism for Cys-loop receptor desensitization. We provided several lines of evidence to support that the balance between coupling strength and gate tightness is the major determinant for uncoupling that underlies receptor desensitization. Thus, loose coupling and tight gating machinery render the α7 nAChR a highly desensitizing receptor. Other previously reported factors such as conditional interactions of N-terminal domain, which may stabilize the receptor in desensitized states, and intracellular domain properties, which may stabilize the receptor in the open states, can also be explained by their indirect influence on coupling. Because this hypothesis can explain many experimental data from other receptor types in the Cys-loop receptor family, it is likely a general mechanism of desensitization in this receptor family.

REFERENCES

1. Chang, Y. C., Wu, W., Zhang, J. L., and Huang, Y. (2009) *Acta Pharmacol. Sin.* **30,** 663–672
2. Chen, Y., Reilly, K., and Chang, Y. (2006) *J. Biol. Chem.* **281,** 18184–18192
3. Changeux, J. P., and Edelstein, S. J. (1998) *Neuron* **21,** 959–980
4. Changeux, J. P. (2010) *Annu. Rev. Pharmacol. Toxicol.* **50,** 1–38
5. Chang, Y., and Weiss, D. S. (2002) *Nat. Neurosci.* **5,** 1163–1168
6. Kash, T. L., Jenkins, A., Kelley, J. C., Trudell, J. R., and Harrison, N. L. (2003) *Nature* **421,** 272–275
7. Lee, W. Y., and Sine, S. M. (2005) *Nature* **438,** 243–247
8. Katz, B., and Thesleff, S. (1957) *J. Physiol.* **138,** 63–80
9. Sakmann, B., Patlak, J., and Neher, E. (1980) *Nature* **286,** 71–73
10. Jones, M. V., and Westbrook, G. L. (1995) *Neuron* **15,** 181–191
11. Giniatullin, R., Nistri, A., and Yakel, J. L. (2005) *Trends Neurosci.* **28,** 371–378
12. Chang, Y., Ghansah, E., Chen, Y., Ye, J., Weiss, D. S., and Chang, Y. (2002) *J. Neurosci.* **22,** 7982–7990
13. Changeux, J. P., Devillers-Thiéry, A., and Chemouilli, P. (1984) *Science* **225,** 1335–1345
14. Hill, D. G., and Baenziger, J. E. (2006) *Biophys. J.* **91,** 705–714
15. Ochoa, E. L., Chattopadhyay, A., and McNamee, M. G. (1989) *Cell Mol. Neurobiol.* **9,** 141–178
16. Paradiso, K. G., and Steinbach, J. H. (2003) *J. Physiol.* **553,** 857–871
17. Quick, M. W., and Lester, R. A. (2002) *J. Neurobiol.* **53,** 457–478
18. Fenster, C. P., Rains, M. F., Noerager, B., Quick, M. W., and Lester, R. A. (1997) *J. Neurosci.* **17,** 5747–5759
19. Gay, E. A., Giniatullin, R., Skorinkin, A., and Yakel, J. L. (2008) *J. Physiol.* **586,** 1105–1115
20. McCormack, T. J., Melis, C., Colón, J., Gay, E. A., Mike, A., Karoly, R., Lamb, P. W., Molteni, C., and Yakel, J. L. (2010) *J. Physiol.* **588,** 4415–4429
21. Bohler, S., Gay, S., Bertrand, S., Corringer, P. J., Edelstein, S. J., Changeux, J. P., and Bertrand, D. (2001) *Biochemistry* **40,** 2066–2074
22. Bouzat, C., Bartos, M., Corradi, J., and Sine, S. M. (2008) *J. Neurosci.* **28,** 7808–7819
23. Hu, X. Q., Sun, H., Peoples, R. W., Hong, R., and Zhang, L. (2006) *J. Biol. Chem.* **281,** 21781–21788
24. Chang, Y., and Weiss, D. S. (1998) *Mol. Pharmacol.* **53,** 511–523
25. Yakel, J. L., Lagrutta, A., Adelman, J. P., and North, R. A. (1993) *Proc. Natl. Acad. Sci. U.S.A.* **90,** 5030–5033
26. Gonzales, E. B., Bell-Horner, C. L., Dibas, M. I., Huang, R. Q., and Dillon, G. H. (2008) *Neurosci. Lett.* **431,** 184–189
27. Placzek, A. N., Grassi, F., Papke, T., Meyer, E. M., and Papke, R. L. (2004) *Mol. Pharmacol.* **66,** 169–177
28. Revah, F., Bertrand, D., Galzi, J. L., Devillers-Thiéry, A., Mulle, C., Hussy, N., Bertrand, S., Ballivet, M., and Changeux, J. P. (1991) *Nature* **353,** 846–849
29. Zhang, J., Xue, F., and Chang, Y. (2008) *Mol. Pharmacol.* **74,** 941–951
30. Zhang, J., Xue, F., and Chang, Y. (2009) *J. Physiol.* **587,** 139–153
31. Hidalgo, P., and MacKinnon, R. (1995) *Science* **268,** 307–310
32. Bouzat, C., Gumilar, F., Spitzmaul, G., Wang, H. L., Rayes, D., Hansen, S. B., Taylor, P., and Sine, S. M. (2004) *Nature* **430,** 896–900
33. Kash, T. L., Dizon, M. J., Trudell, J. R., and Harrison, N. L. (2004) *J. Biol. Chem.* **279,** 4887–4893
34. Miyazawa, A., Fujiyoshi, Y., and Unwin, N. (2003) *Nature* **423,** 949–955
35. Unwin, N. (1995) *Nature* **373,** 37–43
36. Unwin, N. (1993) *J. Mol. Biol.* **229,** 1101–1124
37. Labarca, C., Nowak, M. W., Zhang, H., Tang, L., Deshpande, P., and Lester, H. A. (1995) *Nature* **376,** 514–516
38. Xiu, X., Hanek, A. P., Wang, J., Lester, H. A., and Dougherty, D. A. (2005) *J. Biol. Chem.* **280,** 41655–41666
39. Sala, F., Mulet, J., Sala, S., Gerber, S., and Criado, M. (2005) *J. Biol. Chem.* **280,** 6642–6647
40. Campos-Caro, A., Sala, S., Ballesta, J. J., Vicente-Agulló, F., Criado, M., and Sala, F. (1996) *Proc. Natl. Acad. Sci. U.S.A.* **93,** 6118–6123
41. Bertrand, D., Devillers-Thiéry, A., Revah, F., Galzi, J. L., Hussy, N., Mulle, C., Bertrand, S., Ballivet, M., and Changeux, J. P. (1992) *Proc. Natl. Acad. Sci. U.S.A.* **89,** 1261–1265
42. Keramidas, A., Moorhouse, A. J., Schofield, P. R., and Barry, P. H. (2004) *Prog. Biophys. Mol. Biol.* **86,** 161–204
43. Bocquet, N., Nury, H., Baaden, M., Le Poupon, C., Changeux, J. P., Delarue, M., and Corringer, P. J. (2009) *Nature* **457,** 111–114
44. Hilf, R. J., and Dutzler, R. (2009) *Nature* **457,** 115–118
45. Cymes, G. D., Ni, Y., and Grosman, C. (2005) *Nature* **438,** 975–980
46. Mukhtasimova, N., Free, C., and Sine, S. M. (2005) *J. Gen Physiol.* **126,** 23–39
47. Gleitsman, K. R., Kedrowski, S. M., Lester, H. A., and Dougherty, D. A. (2008) *J. Biol. Chem.* **283,** 35638–35643
48. Lape, R., Colquhoun, D., and Sivilotti, L. G. (2008) *Nature* **454,** 722–727
49. Auerbach, A., and Akk, G. (1998) *J. Gen Physiol.* **112,** 181–197
50. Wilson, G., and Karlin, A. (2001) *Proc. Natl. Acad. Sci. U.S.A.* **98,** 1241–1248